Transactions, SMiRT-24
BEXCO, Busan, Korea - August 20-25, 2017
Division VIII

EFFECT OF MAGNETITE ON SINGLE-PHASE FLOW ACCELERATED CORROSION OF CARBON STEEL IN ALKALINE SOLUTIONS

Geun Dong Song[1], Soon-Hyeok Jeon[2], Yeong-Ho Son[3], Jung Gu Kim[4], Do Haeng Hur[5]

[1] Graduate Student, Materials Research Division, Korea Atomic Energy Research Institute, Korea
[1] Graduate Student, Advanced Materials Science and Engineering, Sungkyunkwan University, Korea
[2] Senior researcher, Materials Research Division, Korea Atomic Energy Research Institute, Korea
[3] Graduate Student, Materials Research Division, Korea Atomic Energy Research Institute, Korea
[4] Professor, Advanced Materials Science and Engineering, Sungkyunkwan University, Korea
[5] Project manager, Materials Research Division, Korea Atomic Energy Research Institute, Korea

ABSTRACT

The objective of this work is to investigate the effect of magnetite on flow accelerated corrosion of carbon steel. Magnetite specimens were prepared by the electrodeposition on the carbon steel substrate in a solution consisted of 2 M sodium hydroxide, 0.1 M triethanolamine and 0.043 M ferric sulphate hydrate. Electrochemical and immersion corrosion tests were carried out in flowing alkaline solutions under a deaerated condition at 60 ºC. The corrosion potential of carbon steel was about 280 ~ 300 mV lower than that of magnetite. This means that carbon steel acts as the anode when carbon steel and magnetite are electrically connected. The corrosion rate of carbon steel was increased by the coupling with magnetite. Furthermore, in this couple, the corrosion of carbon steel was more accelerated with increasing the area ratio of magnetite to carbon steel. The reason why the corrosion rate of carbon steel coupled to magnetite accelerates is that the corrosion potential of carbon steel is shifted in the anodic direction by the galvanic coupling with magnetite.

INTRODUCTION

Flow accelerated corrosion (FAC) causes wall thinning of carbon steel piping and can lead to a catastrophic failure in the secondary circuit system of pressurized water reactors (PWRs) [Hales et al. (2002), Kain et al. (2011)]. The major mechanism of FAC is the increased dissolution of the protective oxide layer on the surface of carbon steel piping under flowing water conditions. The surface of carbon steel piping is normally covered with magnetite layers by the corrosion processes in alkalized reducing conditions of PWRs. These layers are partially removed by flowing water, and the bare metal surface of carbon steel exposed to flowing water is continuously corroded.

Factors affecting the FAC rate have been well identified and quantified: pH [Remy and Bouchacourt (1992)], temperature [Keller (1974)], dissolved oxygen [Fujiwara et al. (2008)], flow velocity [Jonas (1985)], and material composition [Cubicciotti (1988)]. Water chemistry such as pH, dissolved oxygen, and temperature affects the stability of magnetite films, while fluid dynamics affects the mass transfer of soluble iron from the surface of the magnetite film.

Although the effects of various factors mentioned above have been evaluated comprehensively, there is another factor that should be considered in the FAC process. As FAC is progressed, a galvanic cell between the bare metal surface of carbon steel and magnetite can be formed because they are electrically connected. Recently, it has been reported that the corrosion of carbon steel [Jeon et al. (2015), Song et al. (2016)], Alloy 600 [Jeon et al. (2015)] and Alloy 690 [Jeon et al. (2015), Song et al. (2016)] is accelerated when they are galvanically connected with magnetite in various environments. Thus, this galvanic coupling is expected to be an additional acceleration factor on FAC of carbon steel piping. However,

despite the experimental results reported above, the effect of magnetite has still not been considered in evaluating the FAC rate of carbon steel piping.

This work aims to evaluate the effect of magnetite on FAC of carbon steel. To evaluate the corrosion behavior of pure magnetite, the magnetite specimens were prepared by the electrodeposition method. The galvanic corrosion behavior between carbon steel and magnetite was investigated in alkaline solutions by using electrochemical and immersion corrosion tests. According to the mixed potential theory, the galvanic corrosion behavior between carbon steel and magnetite is predicted and its effect on FAC of carbon steel is discussed.

EXPERIMENTAL PROCEDURES

Preparation of Carbon Steel and Magnetite Specimens

Carbon steel specimens were machined from SA106Gr.B pipe material. The detailed dimensions of carbon steel specimen were described in the immersion corrosion test section. The specimens were ground using silicon carbide papers down to grit 1000, and then ultrasonically cleaned in acetone.

Magnetite specimens were prepared by the electrodeposition on the carbon steel substrates using a potentiostat and three-electrode cell. A saturated calomel electrode (SCE) and a pure graphite rod were used as the reference and counter electrodes, respectively. The electrodeposition solutions consisted of 2 M sodium hydroxide, 0.1 M triethanolamine, and 0.043 M ferric sulphate hydrate. The electrodeposition process of magnetite was conducted at an applied potential of -1.05 V_{SCE} at 80 ^{o}C for 1800 s. The detailed electrodeposition process of magnetite is given in previous studies [Kothari et al. (2006), Jeon et al. (2016)]. Characteristics of the magnetite specimen were analyzed using a scanning electron microscope (SEM) and X-ray diffractometer.

Test Solutions

An alkaline aqueous solution of pH 9.5 at 25 ^{o}C was used in this investigation. The pH of the test solution was adjusted using ethanol amine, which is an organic chemical agent used to control the pH of secondary water in PWRs. All corrosion tests were carried out under a deaerated condition at 60 ℃. For the deaerated condition, the test solutions were continuously purged with high-purity nitrogen gas (99.98 %) at a flow rate of 100 cm^3/min during testing. This test environment was designed to simulate a secondary water chemistry of PWRs [Fruzzetti (2009)].

Immersion Corrosion Test

Carbon steel specimens with and without the coupling to magnetite were used in the immersion corrosion test. In case of coupled specimen, the area ratio (AR) of magnetite to carbon steel was controlled to be 1 and 20, respectively. To make the coupled specimens, in case of the AR of 1, square-shaped (20 × 20 × 1 mm^3) carbon steel and magnetite specimens with drilled holes in all corners were prepared as shown in Figure 1(a). These two materials were electrically connected by tightening a polytetrafluoroethylene (PTFE) bolt and nut located at each hole of the specimens. In case of the AR of 20, the disc-shaped (radius: 3.2 mm, thickness: 1 mm) carbon steel specimen with an internal thread in the center and the square-shaped (20 × 20 × 1 mm^3) magnetite with drilled holes in all corners and the center were prepared as shown in Figure 1(b). The carbon steel specimen was located in the center of the magnetite specimen, and then these two materials were electrically connected by tightening a carbon steel bolt. After that, the crevices of these coupled specimens were coated with a water-repellent agent to prevent the permeation of the test solutions, as show in Figure 1. Four coupled samples for each condition were exposed to the test solution for the weight loss measurement and surface analysis.

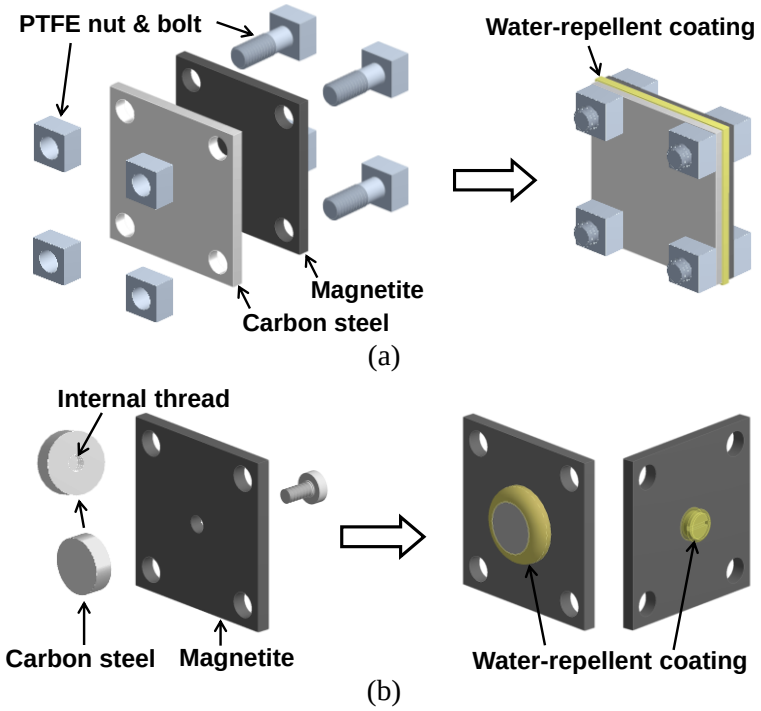

Figure 1. Schematic for the preparation of coupled specimens: (a) AR of 1 and (b) AR of 20.

Figure 2 shows a schematic of the test apparatus for the immersion corrosion test. The test apparatus consisted of a hot plate, water bath, specimen holder, and reaction flask equipped with a reflux condenser, gas sparger, overhead stirrer, and thermocouple. In order to expose all specimens to same fluid dynamic conditions, the samples were placed in each side of a regular dodecagon-shaped specimen holder, which is equidistant 60 mm from the center. After that, the specimen holder was loaded to the end of the overhead stirrer shaft and rotated at a rate of 320 rpm to make a fluid flow at the surface of specimens during the immersion corrosion test. When this angular velocity is converted into a linear velocity, the flow rate of the test solutions at the surface of the specimen is 2 m/s.

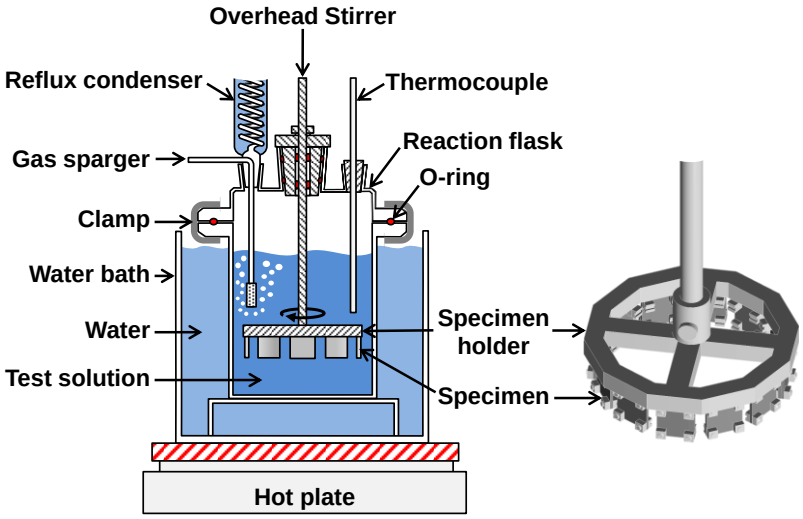

Figure 2. Schematic of the test apparatus for immersion corrosion test.

The immersion corrosion test was conducted for 500 h. After the immersion corrosion test was completed, the samples were ultrasonically cleaned in acetone, and then the weight change of the sample was measured. In addition, the corrosion morphology and surface chemistry of the samples were analyzed using a scanning electron microscope (SEM) and X-ray photoelectron spectroscopy (XPS), respectively.

Electrochemical Corrosion Tests

Potentiodynamic polarization tests were performed using a potentiostat and a three-electrode cell. The SCE and platinum wire were used as a reference and counter electrode, respectively. After the open circuit potential (OCP) was stabilized, polarization scans for carbon steel and magnetite were started from 10 mV below the OCP to the anodic direction or from 10 mV above the OCP to the cathodic direction. The scan rate was 1 mV/s. Each anodic and cathodic polarization curve was finally combined in one graph. In addition, a zero resistance ammeter (ZRA) was used to measure the actual galvanic current density (i_{couple}) and galvanic corrosion potential (E_{couple}) between carbon steel and magnetite. The ARs were 1 and 20. After individual OCPs of carbon steel and magnetite were stabilized, the actual i_{couple} and E_{couple} of the couple was measured for 3600 s. All electrochemical corrosion tests were conducted at least three times to confirm their reproducibility.

RESULTS

Characteristic of the Magnetite Specimen Prepared by the Electrodeposition Method

Figure 3 shows the SEM images of the magnetite specimen prepared by the electrodeposition method. As shown in Figure 3(a), the surface of the electrodeposited magnetite layer had a highly faceted and dense morphology. This magnetite layer was homogeneously electrodeposited over the whole carbon steel substrate. In addition, there were no defects such as crack, pore, or crevice at the interface between the magnetite layer and the substrate, as shown in Figure 3(b). This indicates that the magnetite layer was tightly bonded to the carbon steel substrate. The average thickness of the magnetite layer was approximately 5 μm. In addition, the X-ray diffraction (XRD) patterns of this layer corresponded to pure crystalline magnetite (JCPDS card no. 19-0629). Consequently, this magnetite specimen is very effective to evaluate the electrochemical corrosion behavior of magnetite and its effect on the FAC of carbon steel because only the surface of magnetite is exposed to test solutions, without the exposure of the carbon steel substrate.

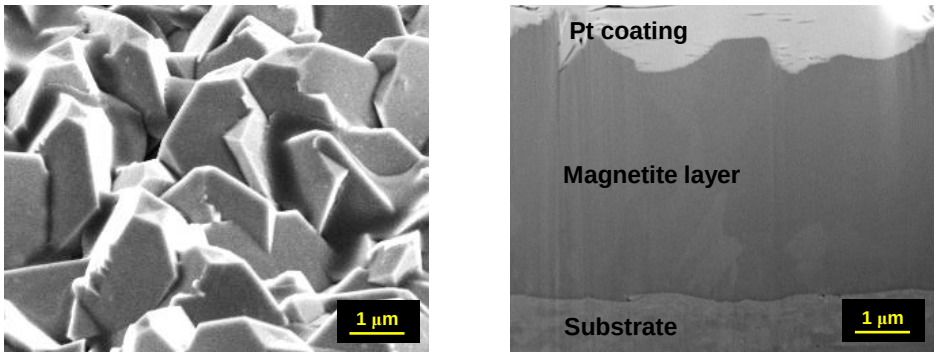

(a) (b)

Figure 3. SEM images of electrodeposited magnetite on the carbon steel substrate at an applied potential of -1.05 V_{SCE} in the electrodeposition solution at 80 ℃ for 1800 s: (a) top view and (b) cross section.

Results of the Immersion Corrosion Test

Figure 4 shows the weight change of carbon steel with and without the coupling to magnetite after the immersion corrosion test in flowing test solutions at a flow velocity of 2 m/s at 60 °C for 500 h. Both carbon steel with and without the coupling to magnetite indicated a weight loss. The weight loss of carbon steel was 0.14 μg/cm^{2}h, while that was significantly increased by the coupling with magnetite. When the AR was 1, the weight loss of carbon steel was increased to 0.30 μg/cm^{2}h. Furthermore, as the AR was increased to 20, the weight loss of carbon steel was drastically increased to 0.86 μg/cm^{2}h. This result indicates that the galvanic coupling with magnetite accelerates the corrosion of carbon steel.

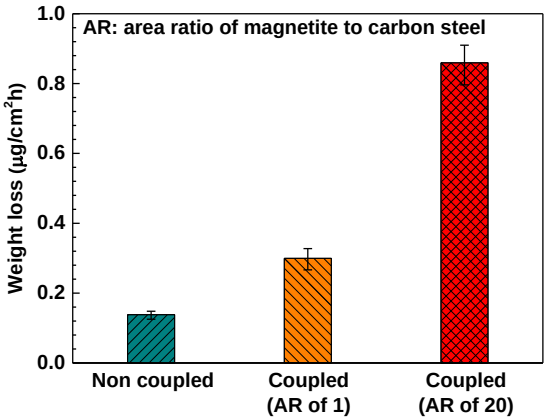

Figure 4. Weight change of carbon steel with and without the coupling to magnetite after the immersion corrosion test in flowing test solutions at a flow velocity of 2 m/s at 60 °C for 500 h.

Figure 5 shows the corrosion morphologies of carbon steel with and without the coupling to magnetite after the immersion corrosion test in flowing test solutions at a flow velocity of 2 m/s at 60 °C for 500 h. The oxide layer formed on the surface of non-coupled carbon steel has a rough morphology. This oxide layer homogeneously formed on the whole carbon steel surface. In case of carbon steel coupled to magnetite with the AR of 1, a relatively smooth oxide layer was uniformly formed on the whole carbon steel surface, compared to non-coupled carbon steel. A few cracks were also observed on the oxide layer. When the AR was increased to 20, the clustered oxide particles were densely formed on the outer layer, and the interstices between them were also observed. These results indicate that the coupling with magnetite affects not only the corrosion rate of carbon steel but also the morphology of the oxide layer formed on that.

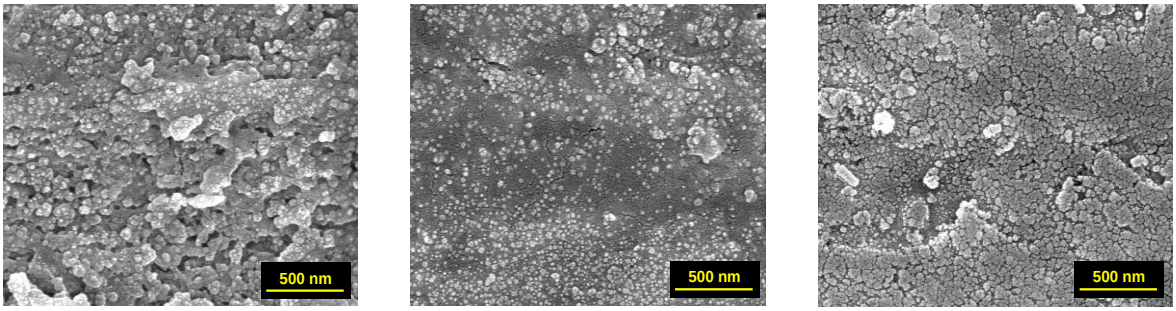

(a) (b) (c)

Figure 5. SEM images of carbon steel with and without the coupling to magnetite after the immersion corrosion test in the flowing test solutions at a flow velocity of 2 m/s at 60 °C for 500 h: (a) non-coupled, (b) AR of 1, and (c) AR of 20.

Figure 6 shows the XPS spectra of Fe2p core-level from the interior of the oxide layer formed on carbon steel with and without the coupling to magnetite after the immersion corrosion test. To analyze the interior of the oxide layer, the surface of the samples was etched using 1.0 keV argon ion beam for 20 s. The Fe2p spectra of the oxide layer for each condition were fitted with peaks corresponding to Fe^{2+} and Fe^{3+}, as shown in Figure 6. The peaks with binding energy at about 709 eV (satellite at 714.8 eV) and 711 eV can be attributed to Fe^{2+} and Fe^{3+} in the oxide form, respectively [Amashita and Hayes (2008), Freire et al. (2009)]. These spectra features were observed in oxide layer formed on carbon steel both with and without the coupling to magnetite, while they showed a difference in the ratios of Fe^{2+} to Fe^{3+} calculated from the deconvoluted spectra. In case of non-coupled carbon steel, the ratio of Fe^{2+} to Fe^{3+} in the oxide form was approximately 0.54. The ratio of Fe^{2+} to Fe^{3+} in stoichiometric magnetite is well known to 0.50 [Cornell (2003)]. Therefore, the oxide layer formed on non-coupled carbon steel seems to be mostly magnetite. The similar tendency was also observed in the oxide layer formed on carbon steel coupled to magnetite with the AR of 1, but the Fe^{3+} contribution in oxide form was slightly increased. However, as shown in Figure 6(c), the spectral feature corresponded Fe^{3+} in oxide form was significantly increased when the AR was increased to 20. The ratio of Fe^{2+} to Fe^{3+} was approximately 0.32. This significant increase of the Fe^{3+} contribution in the oxide form means that the increased area ratio of magnetite to carbon steel results in the oxidation of Fe^{2+} to Fe^{3+} in the oxide layer formed on the surface of carbon steel.

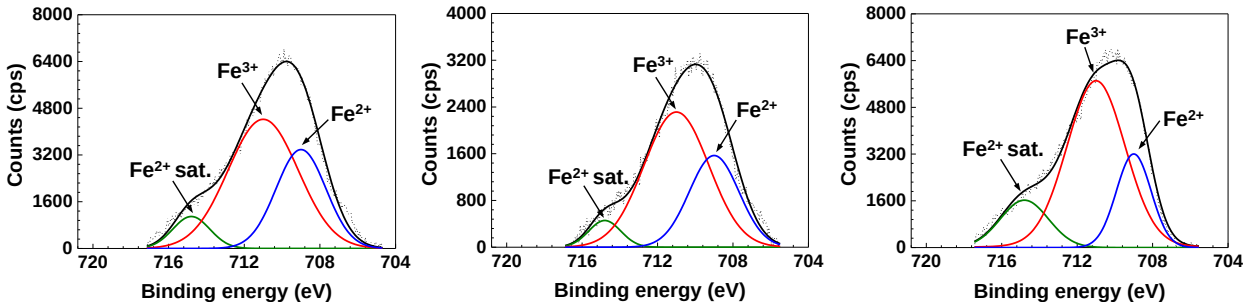

Figure 6. XPS spectra of Fe2p core-level from the interior of the oxide layer formed on the surface of carbon steel with and without the coupling to magnetite after the immersion corrosion test: (a) non-coupled, (b) AR of 1 and (c) AR of 20.

Electrochemical Corrosion Behavior

Figure 7 shows the polarization curves of carbon steel and magnetite, which were measured in the test solutions under deaerated conditions at 60 °C. The corrosion potential (E_{corr}) of carbon steel was about 280 ~ 300 mV lower than that of magnetite. This means that carbon steel and magnetite will act as an anode and cathode, respectively, when these two materials are electrically connected. The anodic current density of carbon steel at the OCP was 1.35 μA/cm^2. That is expected to increase to 8.06 μA/cm^2 if equal areas of carbon steel and magnetite are galvanically coupled. In addition, to evaluate the area effect, polarization curve of magnetite with the area of 20 cm^2 was also presented in Figure 7, which was calculated from that with area of 1 cm^2. When the AR is increased to 20, the anodic current density of carbon steel will increase by about 15-times from 1.35 μA/cm^2 to 21.04 μA/cm^2. These results indicate that an increased area ratio of magnetite to carbon steel accelerates significantly the corrosion of carbon steel because a galvanic attack is concentrated at a small anodic area. Based on the result of polarization tests, the accelerated corrosion of carbon steel by magnetite in Figure 4 is caused by the fact that the galvanic coupling with magnetite shifts the E_{corr} of carbon steel in the anodic direction.

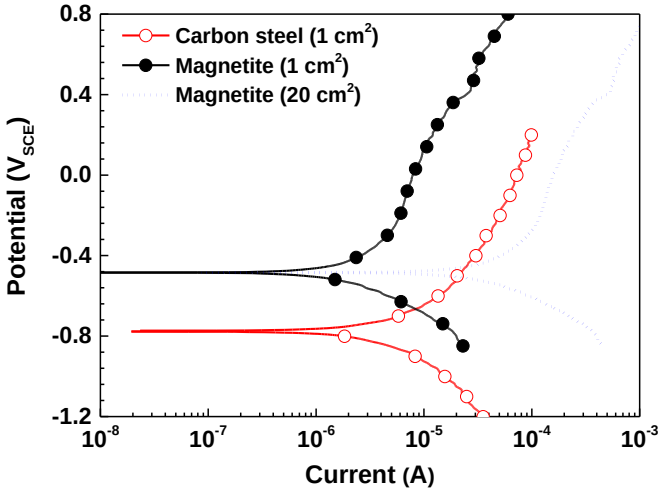

Figure 7. Potentiodynamic polarization curves of carbon steel and magnetite in the test solutions under deaerated conditions at 60 °C

Figure 8 shows the actual E_{couple} and i_{couple} between carbon steel and magnetite obtained from the ZRA measurements in the test solutions under deaerated conditions at 60 °C. As shown in Figure 8(a), both the actual E_{couple} of the couple with the AR of 1 and 20 were located between the E_{corr} of carbon steel and magnetite. The actual E_{couple} of the couple was shifted in the more positive direction with increasing the AR. This means that the increased area ratio of magnetite to carbon steel results in the more oxidizing condition. These changes in the thermodynamic condition can affect the stoichiometry of the oxide layer formed on carbon steel, as shown in Figure 6. Furthermore, the actual i_{couple} of carbon steel coupled to magnetite had an increased anodic current as shown in Figure 8(b), indicating that carbon steel was the anodic member in the galvanic couple with magnetite. When the AR was increased, the actual i_{couple} was increased significantly. These tendencies are in good agreement with results predicted from the mixed potential theory in Figure 7. Therefore, the galvanic corrosion behavior between carbon steel and magnetite can be quantitatively predicted by the application of the mixed potential theory and clearly confirmed using the ZRA technique.

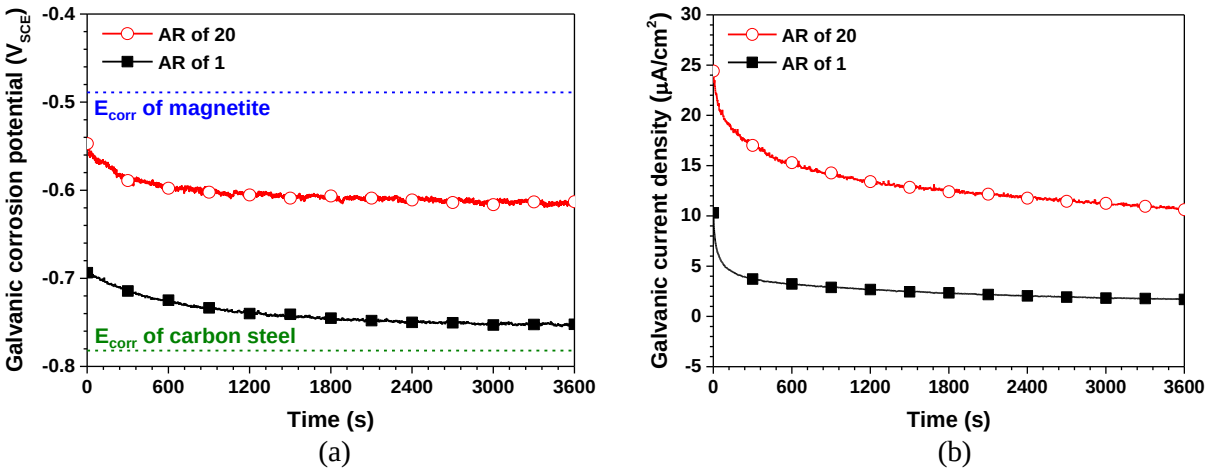

Figure 8. (a) Galvanic corrosion potential and (b) galvanic current density of carbon steel coupled to magnetite obtained from the ZRA measurements in the test solutions under deaerated conditions at 60 °C

DISCUSSION

The results obtained in this work can be summarized as follows: the corrosion of carbon steel was accelerated by the galvanic coupling with magnetite. A large area ratio of magnetite to carbon steel more accelerated the corrosion of carbon steel. In addition, the morphology and stoichiometry of oxide layer formed on carbon steel were significantly changed by the galvanic coupling with magnetite. This accelerated corrosion of carbon steel by magnetite can be discussed as an acceleration factor on FAC mechanism occurring in the secondary system of PWRs.

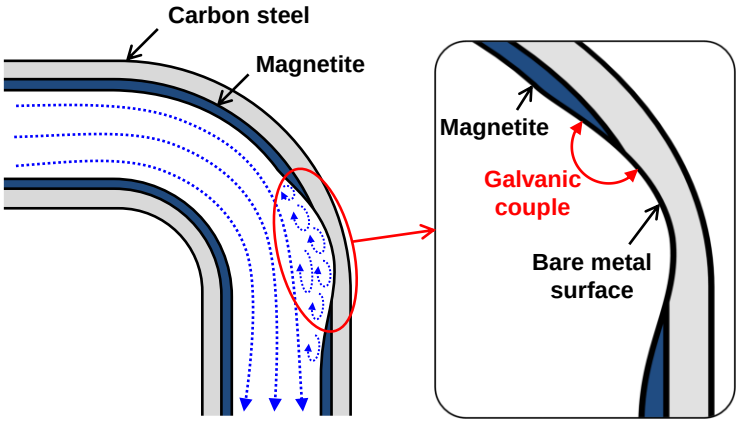

Figure 9. Schematic for galvanic corrosion between carbon steel and magnetite occurring in a pipe bend during FAC process.

The surface of carbon steel piping is typically covered with the protective magnetite layer under alkalized reducing conditions of PWRs. FAC has been known to be a simple mass-transfer process that the dissolution of this magnetite layer on carbon steel is accelerated by flowing water. This type of corrosion is most severe in regions such as elbows, tees and bends where the pattern of the turbulent flow changes. These areas are expected to contain very thin magnetite layer remaining on the surface, and expose the metal surface [Nasrazadani et al. (2009)]. In this situation, the bare metal surface of carbon steel is electrically connected with the remaining magnetite layer, as shown in Figure 9. That is, the galvanic corrosion can be occurred between carbon steel and magnetite during the FAC process.

This paper provides a new additional mechanism by magnetite on flow accelerated corrosion of carbon steel. The experimental result simulating the situation as Figure 9 shows that the coupling with magnetite accelerated the corrosion of carbon steel, as shown in Figure 4. In addition, the electrochemical behavior of magnetite and carbon steel demonstrates that the corrosion of carbon steel is accelerated by a galvanic corrosion mechanism based on the mixed potential theory in Figure 7. This corrosion mechanism can be supported by the results obtained from ZRA measurements in Figure 8. Furthermore, under operating conditions of PWRs, the local areas of carbon steel piping occurring FAC are in the condition of an unfavorably large area ratio of the magnetite to carbon steel. It is clearly verified that the corrosion of carbon steel was more accelerated with increasing the area ratio of magnetite to carbon steel in the results of immersion and electrochemical corrosion tests in Figures 4, 7 and 8. Thus, wall thinning of carbon steel piping by FAC will be more accelerated owing to the galvanic corrosion mechanism described above under operating conditions of PWRs.

In this work, the accelerated corrosion of carbon steel by the galvanic coupling with magnetite was clearly confirmed using immersion and electrochemical corrosion tests at 60 ^{o}C. Therefore, we propose that the galvanic effect with magnetite must be considered in evaluating the FAC of carbon steel as an additional acceleration factor. Further, the extent of galvanic corrosion depends on the difference in the OCPs and the polarization behavior of the coupled materials, which is affected by temperature. Thus,

extensive experimental works are ongoing to validate the galvanic effect in the high temperature ranges up to 230 °C.

CONCLUSIONS

(1) To evaluate the effect of magnetite on FAC of carbon steel, the magnetite specimen was prepared by the electrodeposition method. This method is easy to produce the adherent magnetite on the carbon steel substrate. In addition, adherent magnetite specimens are effective to study the electrochemical behavior of magnetite.

(2) The weight loss of carbon steel was increased by the coupling with magnetite. A large area ratio of magnetite to carbon steel increased more the weight loss of carbon steel. In addition, the coupling with magnetite influenced the morphology and the stoichiometry of the oxide layer formed on carbon steel.

(3) The E_{corr} of carbon steel was lower than that of magnetite. This demonstrates that carbon steel and magnetite play the role of anode and cathode, respectively, if they are electrically contacted. In this galvanic couple, the corrosion current of carbon steel increased significantly.

(4) Based on the results of electrochemical and immersion corrosion tests, the galvanic corrosion between carbon steel and magnetite is proposed as an additional acceleration factor on FAC of carbon steel piping in the secondary circuit system of PWRs.

ACKNOWLEDGMENT

This work was supported by the National Research Foundation of Korea (NRF) grant funded by the Korea government (MSIP) (2017M2A8A4015159).

REFERENCES

Cornell, R. M. (2003). *The Iron oxides: Structure, Properties, Reactions, Occurrences and Uses, 2nd ed*., Wiley-VCH GmbH & Co. KGaA.

Cubicciotti, D. (1988). "Flow-Assisted Corrosion of Steel and the Influence of Cr and Cu Additions," *Journal of Nuclear Materials*, NLD, 152 259-264.

Freirea, L., Nóvoaa, X.R., Montemorb, M.F., Carmezimb, M.J., (2009). "Study of Passive Films Formed on Mild Steel in Alkaline Media by the Application of Anodic Potentials," *Materials Chemistry and Physics*, CH, 114 962–972.

Fruzzetti, K. (2009). "Pressurized Water Reactor Secondary Water Chemistry Guidelines-Revision 7," Electric Power Research Institute, EPRI TR-1016555.

Fujiwara, K., Domae, M., Ohira, T., Hisamune, K., Takiguchi, H., Uchida, S. and Lister, D. (2008). "Electrochemical Measurements of Carbon Steel under high Flow Rate Condition and Thermodynamic Solubility of Iron," *Proc., 16th Pacific Basin Nuclear Conference*, AESJ, Tokyo, JP, Paper No. P16P1048.

Hales, C., Stevens, K. J., Daniel, P. L., Zamanzadeh, M., Owens, A. D. (2002). "Boiler Feedwater Pipe Failure by Flow-Assisted Chelant Corrosion," *Engineering Failure Analysis*, UK, 9 235-243.

Jeon, S. H., Song, G. D., Hur, D. H. (2015). "Electrodeposition of Magnetite on Carbon Steel in Fe(III)-Triethanolamine Solution and its Corrosion Behavior," *Materials transactions*, JP, 56 1107-1111.

Jeon, S. H., Song, G. D., Hur, D. H. (2015). "Corrosion Behavior of Alloy 600 Coupled with Electrodeposited Magnetite in Simulated Secondary Water of PWRs," *Materials transactions*, JP, 56 2078-2083.

Jeon, S. H., Song, G. D., Hur, D. H. (2015). "Galvanic Corrosion between Alloy 690 and Magnetite in Alkaline Aqueous Solutions," *Metals*, CH, 5 2372-2382.

Jeon, S. H., Song, G. D., Hur, D. H. (2016). "Effects of Deposition Potentials on the Morphology and Structure of Iron-Based Films on Carbon Steel Substrate in an Alkaline Solution," *Advances in Materials Science and Engineering*, USA, 2016 Article ID 9038478.

Jonas, O. (1985). "Control Erosion/corrosion of Steels in Wet Steam," *Power*, USA, 129 102-103.

Kain, V., Roychowdhury, S., Ahmedabadi, P., Barua, D. K. (2011). "Flow Accelerated Corrosion: Experience from Examination of Components from Nuclear Power Plants," *Engineering Failure Analysis*, UK, 18 2028-2041.

Keller, V. H. (1974). "Erosion Corrosion in Damp Steam Turbine," *VGB Kraftwerkstechnik*, DE, 54 292

Kothari, H. M., Kulp, E. A., Limmer, S. J., Poizot, P., Bohannan, E. W., Switzer, J. A. (2006). "Electrochemical Deposition and Characterization of Fe_3O_4 Films Produced by The Reduction of Fe (III)-Triethanolamine," *Journal of materials research*, USA, 21 293-301.

Nasrazadani, S., Nakka, R. K., Hopkins, D., Stevens, J. (2009). "Characterization of Oxides on FAC Susceptible Small-Bore Carbon Steel Piping of a Power Plant," *International Journal of Pressure Vessels and Piping*, UK, 86 845-852.

Remy, F. N., Bouchacourt, M. (1992). "Flow-assisted Corrosion: a Method to Avoid Damage," *Nuclear Engineering and design*, UK, 133 23-30.

Song, G. D., Jeon, S. H., Kim, J. G., Hur, D. H. (2016). "Effect of Polyacrylic Acid on the Corrosion Behavior of Carbon Steel and Magnetite in Alkaline Aqueous Solutions," *Corrosion*, USA, 72 1010-1020.

Song, G. D., Jeon, S. H., Kim, J. G., Hur, D. H. (2017). "Synergistic Effect of Chloride Ion and Magnetite on the Corrosion of Alloy 690 in Alkaline Solutions," *Corrosion*, USA, 73 216-220.

Yamashita, T., Hayes, P. (2008). "Analysis of XPS Spectra of Fe^{2+} and Fe^{3+} Ions in Oxide Materials," *Applied Surface Science*, NLD, 254 2441-2449.